

# Evidence for the bipolaron formation in the paramagnetic state of the magnetoresistive manganites

Guo-meng Zhao<sup>(1,2)</sup>, Y. S. Wang<sup>(3)</sup>, D. J. Kang<sup>(1)</sup>, W. Prellier<sup>(1,\*)</sup>, M. Rajeswari<sup>(1)</sup>,

H. Keller<sup>(2)</sup>, T. Venkatesan<sup>(1)</sup>, C. W. Chu<sup>(3)</sup>, and R. L. Greene<sup>(1)</sup>

<sup>(1)</sup>*Center for Superconductivity Research, University of Maryland, College Park, MD 20742, USA*

<sup>(2)</sup>*Physik-Institut der Universität Zürich, CH-8057 Zürich, Switzerland*

<sup>(3)</sup>*Department of Physics and Texas Center for Superconductivity, University of Houston, Houston, Texas 77204, USA*

Recent research suggests that the charge carriers in the paramagnetic state of the magnetoresistive manganites are small polarons. Here we report studies of the oxygen-isotope effects on the intrinsic resistivity and thermoelectric power in several ferromagnetic manganites. The precise measurements of these isotope effects allow us to make a quantitative data analysis. Our results do not support a simple small-polaron model, but rather provide compelling evidence for the presence of small bipolarons, i.e., pairs of small polarons.

The discovery of “colossal” magnetoresistance (CMR) in thin films of  $Re_{1-x}A_xMnO_3$  ( $Re$  = a rare-earth element, and  $A$  = a divalent element) [1] has stimulated extensive studies of magnetic, structural and transport properties of these materials [2]. The physics of manganites has primarily been described by the double-exchange (DE) model [3]. However, Millis, Littlewood and Shraiman [4] pointed out that the carrier-spin interaction in the DE model is too weak to lead to carrier localization in the paramagnetic (PM) state, and thus a second mechanism such as small polaronic effects should be involved to explain the observed resistivity data in doped manganites. Following this original idea, more theoretical models were proposed [5,6]. On the other hand, Alexandrov and Bratkovsky [7] have recently shown that the essential physics in manganites should involve the formation of small bipolarons in the PM state in order to explain CMR quantitatively.

The first experimental evidence for small polaronic charge carriers in the PM state was provided by transport measurements [8]. It was found that the activation energy  $E_\rho$  deduced from the conductivity data is one order of magnitude larger than the activation energy  $E_s$  obtained from the thermoelectric power data. Such a large difference in the activation energies is the hallmark of the small-polaron hopping conduction. The giant oxygen-isotope shifts of the ferromagnetic transition temperature  $T_C$  give clear evidence for the presence of polaronic charge carriers in this system [9,10]. Moreover, the fast and local techniques have directly shown that the doped charge carriers are accompanied by local Jahn-Teller distortions [11–14]. However, all these experiments cannot make a distinction between small polarons and small bipolarons since both are dressed by local lattice distortions. Small bipolarons are normally much heavier than small polarons, and should be localized in the presence of small random potentials. In or-

der to discriminate between polarons and bipolarons and to place constraints on the CMR theories, we studied the oxygen-isotope effects on the intrinsic resistivity in the high-quality epitaxial thin films of  $La_{0.75}Ca_{0.25}MnO_3$  and  $Nd_{0.7}Sr_{0.3}MnO_3$ . We also measured the thermoelectric power for the oxygen-isotope exchanged ceramic samples of  $La_{0.75}Ca_{0.25}MnO_3$ . The data cannot be explained by a simple small-polaron model, but are in quantitative agreement with a model where the formation of small bipolarons is essential.

The epitaxial thin films of  $La_{0.75}Ca_{0.25}MnO_3$  (LCMO) and  $Nd_{0.7}Sr_{0.3}MnO_3$  (NSMO) were grown on  $<100> LaAlO_3$  single crystal substrates by pulsed laser deposition using a KrF excimer laser [15]. The film thickness was about 190 nm for NSMO and 150 nm for LCMO. Two halves were cut from the same piece of a film for oxygen-isotope diffusion. The diffusion for LCMO/NSMO was carried out for 10 h at about 940/900 °C and oxygen pressure of 1 bar. The  $^{18}O$ -isotope gas is enriched with 95%  $^{18}O$ , which can ensure 95%  $^{18}O$  in the  $^{18}O$  thin films. The ceramic  $^{16}O$  and  $^{18}O$  samples of  $La_{0.75}Ca_{0.25}MnO_3$  were the same as those reported in Ref. [16]. The resistivity was measured using the van der Pauw technique, and the contacts were made by silver paste. The measurements were carried out in a Quantum Design measuring system. The thermoelectric power was measured using an apparatus modeled after a seesaw technique [17]. The absolute uncertainty is less than 0.25  $\mu V/K$  and the systematic error is  $\pm 0.1 \mu V/K$ .

Fig. 1 shows the resistivity of the oxygen-isotope exchanged LCMO films above  $1.1T_C$ , where  $T_C = 231.5$  K for the  $^{16}O$  sample and 216.5 K for the  $^{18}O$  sample (see Table 1). The oxygen-isotope shift of  $T_C$  is 15.0(6) K in the films, in excellent agreement with the results for the bulk samples [16]. From the figure, one can see that there is a large difference in the intrinsic resistivity between the two isotope samples. Such a large isotope ef-

fect is reversible upon the oxygen isotope back-exchange. We should mention that the intrinsic resistivity of the compounds can be only obtained in high-quality thin films and single crystals. Our LCMO films even have lower residual resistivity  $\rho_o$  than the corresponding single crystals [18], indicating a high-quality of the films. We also checked that the resistivity for a ceramic sample of  $\text{La}_{0.66}\text{Ba}_{0.34}\text{MnO}_3$  is very different from that for the corresponding single crystal; the activation energy  $E_\rho$  for the former is about 3 times larger than for the latter. The temperature dependence of the resistivity obtained in the ceramic samples does not represent the intrinsic behavior of the bulk, and thus one cannot use ceramic samples to study the isotope effect on the intrinsic resistivity. Moreover, the van der Pauw technique is particularly good to precisely measure the resistivity difference between oxygen-isotope exchanged films whose thicknesses are identical. Thus the data shown in Fig. 1 represent the first precise measurements on the intrinsic resistivity of the two isotope samples.

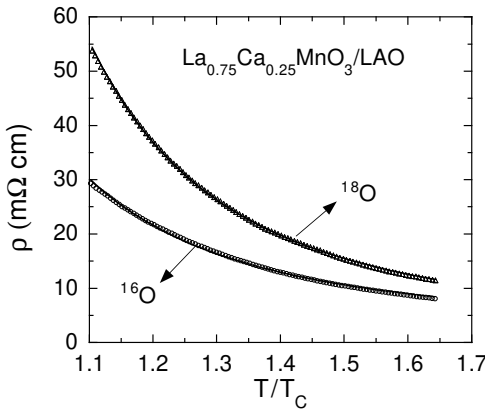


FIG. 1. The resistivity of the oxygen-isotope exchanged films of  $\text{La}_{0.75}\text{Ca}_{0.25}\text{MnO}_3$ . The maximum temperature of the data points for the  $^{16}\text{O}$  film is 380 K. The solid lines are the fitted curves by Eq. 1. As in Ref. [8], we excluded the data points below  $1.1T_C$  for the fitting.

In the PM state, the dominant conduction mechanism is thermally activated hopping of adiabatic small polarons. When  $T > W_p/k_B$  (where  $W_p$  is the polaron bandwidth), the temperature dependence of the resistivity is given by [19,20,8]

$$\rho = BT \exp[(E_a + E_s)/k_B T], \quad (1)$$

where  $B$  is a coefficient, depending on a characteristic optical phonon frequency  $\omega_o$  (i.e.,  $B \propto 1/\omega_o$ );  $E_s$  is the energy required to excite a polaron from a localized impurity state (see Fig. 2a);  $E_a = (\eta E_p/2) - t$  (here  $E_p$  is the polaron binding energy,  $t$  is the “bare” hopping integral,  $\eta = 1$  for Holstein polarons [19] and  $\eta \sim 0.2\text{--}0.4$  for Fröhlich polarons [21]). In the harmonic approximation,  $E_p$  and  $E_a$  are independent of the isotope mass  $M$ .

Moreover, since  $E_s$  does not depend on  $M$  either [20], one expects that  $E_\rho = E_a + E_s$  should be independent of  $M$ .

The thermoelectric power is given by [8,20]

$$S = E_s/eT + S_o \quad (2)$$

where  $S_o$  is a constant depending on the kinetic energy of the polarons and on the polaron density [20]. One should note that Eq. 2 is valid only if there is one type of carriers (e.g., holes). Comparing Eq. 1 and Eq. 2, one readily finds that  $E_\rho = E_a + E_s >> E_s$ . Jaime *et al.* [8] used the above equations to fit their resistivity and thermoelectric power data, and found that  $E_\rho >> E_s$ . This is consistent with the small polaron hopping mechanism.

We now fit our data by Eq. 1 (see solid lines in Fig. 1). It is apparent that the fits are quite good for both isotope samples. However, the isotope dependencies of the parameters  $B$  and  $E_\rho$  are not expected from Eq. 1. Upon replacing  $^{16}\text{O}$  with  $^{18}\text{O}$ , the parameter  $B$  decreases by 20%, and the parameter  $E_\rho$  increases by 11 meV. This is in contradiction with Eq. 1 which predicts that the parameter  $B$  should increase by about 6% while  $E_\rho$  should not change. Since our measurements are very accurate, the unusual isotope effect on  $B$  cannot be caused by the experimental uncertainty. One possible explanation is that Eq. 1 does not hold below 380 K (the maximum temperature of the data points in Fig. 1) since the condition  $T > W_p/k_B$  may not be satisfied in this system.

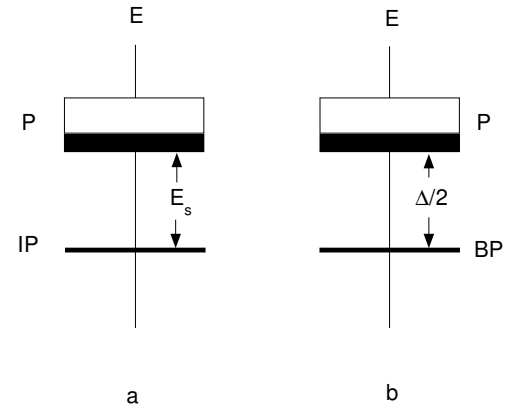


FIG. 2. A schematic diagram of the polaron band, and polaron trapping into impurity (IP) states (a), or into localized bipolaron (BP) states (b).

One should modify Eq. 1 if  $T < W_p/k_B$ . It is known that the resistivity can be generally expressed as  $\rho = 1/\sigma = 1/ne\mu$ , where  $n$  is the mobile carrier concentration and  $\mu$  is the mobility of the carriers. For adiabatic small-polaron hopping, the mobility is given by [19]

$$\mu = \frac{ed^2}{h} \frac{\hbar\omega_o}{k_B T} \exp(-E_a/k_B T), \quad (3)$$

where  $d$  is the site to site hopping distance, which is equal to  $a/\sqrt{2}$  in manganites since the doped holes

in this system mainly reside on the oxygen sites [23]. Here  $E_a$  should also be modified at low temperatures [20], i.e.,  $E_a = (\eta E_p/2)f(T) - t$ , where  $f(T) = [\tanh(\hbar\omega_o/4k_B T)]/(\hbar\omega_o/4k_B T)$  for  $T > \hbar\omega_o/4k_B \simeq 200$  K [20]. The mobile polaron density  $n$  can be easily calculated with the help of Fig. 2. When  $T > W_p/k_B$ ,  $n \propto \exp(-E_s/k_B T)$  [20], which leads to Eq. 1 by combining with Eq. 3. On the other hand, when  $T < W_p/k_B$ ,  $n = 2(2\pi m_p k_B T/\hbar^2)^{3/2} \exp(-E_s/k_B T)$  if we assume a simple parabolic band [7,20]. Here  $m_p$  is the effective mass of polarons and related to  $W_p$  by  $m_p = 6\hbar^2/a^2 W_p$ . In fact, the above  $n(T)$  expression is the same as that for semiconductors when the chemical potential is pinned to the impurity levels. Using the above  $n(T)$  expression in the case of  $T < W_p/k_B$  and Eq. 3, we finally have

$$\rho = \frac{C}{\sqrt{T}} \exp(E_\rho/k_B T), \quad (4)$$

where  $C = (ah/e^2\sqrt{k_B})(1.05W_p)^{1.5}/\hbar\omega_o$ . The quantity  $C$  should strongly depend on the isotope mass  $M$  and de-

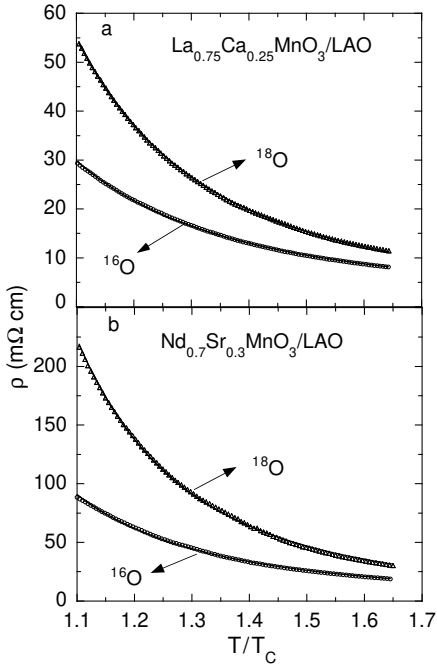


FIG. 3. The resistivity of the oxygen-isotope exchanged films of (a)  $\text{La}_{0.75}\text{Ca}_{0.25}\text{MnO}_3$ ; (b)  $\text{Nd}_{0.7}\text{Sr}_{0.3}\text{MnO}_3$ . The solid lines are fitted curves by Eq. 4.

crease with increasing  $M$ . This is because  $W_p$  decreases strongly with increasing  $M$  according to  $W_p = W_o \exp(-\Gamma E_p/\hbar\omega_o) = W_o \exp(-g^2)$  [22,21]. Here  $W_o$  is the bare bandwidth ( $W_o = 12t$ ),  $\Gamma$  is an isotope independent constant, which is less than 0.4 for both Holstein and Fröhlich polarons when the coupling constant  $\lambda = 2E_p/W_o < 0.5$  and  $\hbar\omega_o/t < 1$  [22]. Clearly, the parameter  $C$  should decrease significantly with increasing

oxygen-isotope mass, in contrast to the parameter  $B$  ( $\propto 1/\omega_o$ ) which would increase by about 6% upon replacing  $^{16}\text{O}$  with  $^{18}\text{O}$ .

Now If one considers that small polarons are bound into localized bipolarons [7], the only modification for both Eq. 2 and Eq. 4 is to replace  $E_s$  by  $\Delta/2$  (see Fig. 2). Here  $\Delta$  is the bipolaron binding energy and given by  $\Delta = 2E_p - V_c - W_p$ , where  $V_c$  is the Coulombic repulsion between bound polarons [7]. It is apparent that  $\Delta$  and thus  $E_s$  should depend on the isotope mass  $M$  due to the fact that  $W_p$  is a strong function of  $M$ .

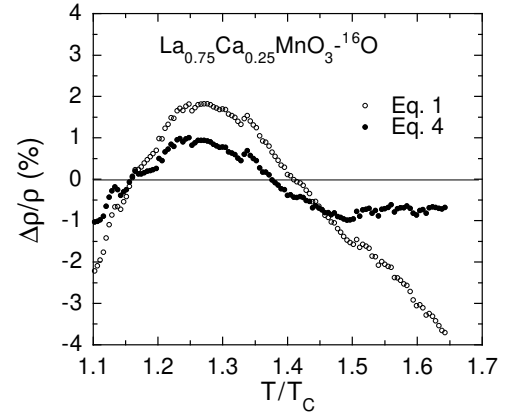


FIG. 4. The deviations between the data of the  $^{16}\text{O}$  film of  $\text{La}_{0.75}\text{Ca}_{0.25}\text{MnO}_3$  and the fitted curves by Eq. 1 and Eq. 4.

In Fig. 3, we show the resistivity data for the  $^{16}\text{O}$  and  $^{18}\text{O}$  films of both LCMO and NSMO compounds, and fit them by Eq. 4. The data can be well fitted by Eq. 4 with the parameters summarized in Table I. It is striking that the fits with Eq. 4 are much better than the fits with Eq. 1, as seen more clearly in Fig. 4 where the deviations between the data and the fitted curves are plotted for the LCMO  $^{16}\text{O}$  film. The fit with Eq. 1 has a large systematic deviation ( $>4\%$ ), while the fit with Eq. 4 has a much smaller deviation ( $<1\%$ ). It is easy to check that the  $T$  dependence of the prefactor of the exponential function in Eq. 1 and Eq. 4 is not important when  $E_\rho$  is large, but becomes crucial when  $E_\rho$  is small. This can naturally explain why the resistivity data in the  $\text{La}_{1-x}\text{Ca}_x\text{MnO}_3$  system can be well fitted by Eq. 1, but the data of the  $\text{La}_{0.7}\text{Sr}_{0.3}\text{MnO}_3$  film are not consistent with Eq. 1 [24]. We speculate that the data of  $\text{La}_{0.7}\text{Sr}_{0.3}\text{MnO}_3$  in Ref. [24] should be in agreement with Eq. 4.

From Table I, one can see that the the parameter  $C$  for LCMO decreases by 35(5)%, and  $E_\rho$  increases by 13.2(3) meV. For NSMO,  $C$  decreases by 40(7)%, and  $E_\rho$  increases by 14.2(8) meV. The deduced oxygen-isotope effects on the parameter  $C$  and  $E_\rho$  are in qualitative agreement with Eq. 4. Since this equation is valid independent of whether the small polarons are bound into localized bipolarons or to the impurity centers (see Fig. 2 and discussion above), one can only draw a conclusion that the

isotope dependence of the electrical transport in the PM state of the manganites agrees qualitatively with small polaron hopping conduction.

Now the question arises: Can the present data tell whether the small polarons are bound into localized bipolarons or to the impurity centers? The clarification of this issue can place an essential constraint on various CMR theories. If the small polarons are bound to impurity centers, there will be no isotope effect on  $E_s$  [20]. Then, the isotope effect on  $E_\rho$  only arises from the isotope shift of  $E_a$  because  $E_\rho = E_a + E_s$ . Since  $E_a = (\eta E_p/2)f(T) - W_o/12$ , only the quantity  $f(T) = [\tanh(\hbar\omega_o/4k_B T)]/(\hbar\omega_o/4k_B T)$  may depend on the isotope mass if the temperature is not so high compared with  $\hbar\omega_o/k_B$ . If we take  $\hbar\omega_o = 74$  meV, typical for oxides [22], we have  $f(T) = 0.855$  and the isotope-induced change  $\delta f(T) = 0.0134$  at  $T = 300$  K, the mid-point temperature of the data points for the LCMO films. Using the relation:  $(\eta E_p/2)f(T) = W_o/12 + E_\rho - E_s$ , and  $E_s = 13.2$  meV for  $\text{La}_{0.75}\text{Ca}_{0.25}\text{MnO}_3$  (see below), we find  $\eta E_p/2 = 0.55$  eV. Here we have used  $W_o = 4.9$  eV, as estimated from the relation:  $W_o = 6\hbar^2/a^2 m_b$  and  $m_b = 0.61 m_e$  [25]. The estimated bare bandwidth is typical for the oxygen band and in good agreement with the electron-energy-loss spectra [23]. Then  $\delta E_\rho = \delta E_a = (\eta E_p/2)\delta f(T) = 7.4$  meV, which is about half the value observed. This implies that there must be an isotope effect on  $E_s$ , which is only possible if the small polarons are bound into localized bipolarons as discussed above. The oxygen-isotope shift of  $E_s$  in the LCMO compound is  $\delta E_s = \delta E_\rho - \delta E_a = 5.8(3)$  meV.

One can also obtain the isotope shift of  $E_s$  by measuring the thermoelectric power for two isotope samples according to Eq. 2. In Fig. 5, we plot the thermoelectric power  $S$  as a function of  $1/T$  for the  $^{16}\text{O}$  and  $^{18}\text{O}$  samples of  $\text{La}_{0.75}\text{Ca}_{0.25}\text{MnO}_3$ . Both  $T_C$ 's and the isotope shift of the ceramic samples [16] are the same as those in the corresponding thin films. Since the grain-boundary effect on  $S$  is negligible, the thermoelectric power obtained in ce-

TABLE I. Summary of the fitting and measured parameters for the  $^{16}\text{O}$  and  $^{18}\text{O}$  films of  $\text{La}_{0.75}\text{Ca}_{0.25}\text{MnO}_3$  (LCMO) and  $\text{Nd}_{0.7}\text{Sr}_{0.3}\text{MnO}_3$  (NSMO). The errors of the parameters comes from the fitting and from the van der Pauw measurement. The absolute uncertainty of the thickness of the films was not included in the error calculations since it only influences the absolute values of the resistivity.

Compounds	$T_C$ (K)	$\rho_0$ ( $\mu\Omega\text{cm}$ )	$C$ ( $\text{m}\Omega\text{cmK}^{0.5}$ )	$E_\rho$ (meV)
LCMO( $^{16}\text{O}$ )	231.5(3)	122(2)	17.3(5)	72.8(2)
LCMO( $^{18}\text{O}$ )	216.5(3)	149(3)	12.9(3)	86.0(1)
NSMO( $^{16}\text{O}$ )	204(1)	248(5)	23.2(8)	78.8(4)
NSMO( $^{18}\text{O}$ )	186(1)	289(5)	16.2(7)	92.9(4)

ramic samples should be intrinsic. From the slopes of the straight lines in Fig. 5, we find  $E_s = 13.2$  meV for the  $^{16}\text{O}$  sample and 18.7 meV for the  $^{18}\text{O}$ . The isotope shift is  $\delta E_s = 5.5(5)$  meV, in remarkably good agreement with that (5.8 meV) deduced independently from the above resistivity data.

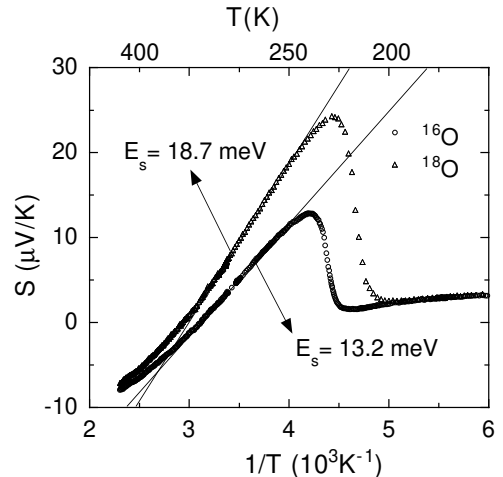


FIG. 5. The thermoelectric power  $S(T)$  of the oxygen-isotope exchanged ceramic samples of  $\text{La}_{0.75}\text{Ca}_{0.25}\text{MnO}_3$ .

We can use the values of the parameter  $C$  for the  $^{16}\text{O}$  films to calculate the polaron bandwidth  $W_p$  according to the relation:  $C = (ah/e^2\sqrt{k_B})(1.05W_p)^{1.5}/\hbar\omega_o$ . By taking  $\hbar\omega_o = 74$  meV, we obtain  $W_p = 49(2)$  meV for the LCMO  $^{16}\text{O}$  film, and 60(3) meV for the NSMO  $^{16}\text{O}$  film. A larger  $W_p$  for the NSMO film might be an artifact since the residual resistivity  $\rho_o$  of this film is about 40% larger than that of the best single crystal [26]. The discrepancy is possibly due to the fact that the interdiffusion between the NSMO film and substrate might occur during the high-temperature anneal. From the  $W_p$  values, one can see that for our data  $T < W_p/k_B$ , which justifies the use of Eq. 4. Moreover, the polaron bandwidth is greatly reduced compared with the bare bandwidth  $W_o = 4.9$  eV. Using  $g^2 = \ln(W_o/W_p)$ , we can determine  $g^2$  to be 4.6(1)/4.4(3) for the LCMO/NSMO  $^{16}\text{O}$  film. If  $\hbar\omega_o$  decreases by 5.7% upon replacing  $^{16}\text{O}$  by  $^{18}\text{O}$ , then our calculation shows that the parameter  $C$  decreases by 35% for LCMO, and by 33% for the NSMO, in good agreement with the measured values: 35(5)% for LCMO and 40(7)% for NSMO.

Furthermore, one can quantitatively explain the isotope dependence of  $E_\rho$  if small polarons form localized bipolarons. In this scenario,  $\delta\Delta = -\delta W_p$  (see above), so  $\delta\Delta = 0.057g^2W_p$ . From the deduced values for  $g^2$  and  $W_p$  above, we calculate that  $\delta\Delta = 12.9$  meV for LCMO, and 15.0 meV for NSMO. So  $\delta E_s = \delta\Delta/2 = 6.5$  meV for LCMO, in quantitative agreement with the values deduced independently from both resistivity and thermoelectric power data. Using  $\delta E_\rho = \delta E_a + \delta\Delta/2$ ,

we find  $\delta E_\rho = 13.8$  meV for LCMO, and 15.3 meV for NSMO. The calculated values are in excellent agreement with the observed values: 13.2(3) meV for LCMO and 14.2(8) meV for NSMO.

In summary, we have observed large oxygen isotope effects on the intrinsic resistivity in high-quality epitaxial thin films of  $\text{La}_{0.75}\text{Ca}_{0.25}\text{MnO}_3$  and  $\text{Nd}_{0.7}\text{Sr}_{0.3}\text{MnO}_3$ , and on the thermoelectric power in the ceramic samples of  $\text{La}_{0.75}\text{Ca}_{0.25}\text{MnO}_3$ . The data can be quantitatively explained by a scenario [7] where the small polarons form localized bound pairs (bipolarons) in the paramagnetic state. The coexistence of small polarons and bipolarons in the PM state may lead to a dynamic phase separation into the insulating antiferromagnetically coupled region where the bipolarons reside, and into the metallic ferromagnetically coupled region where the polarons sit. This simple picture can naturally explain the observation of the ferromagnetic clusters in the PM state [27]. Although we cannot completely rule out the possibility that the other models might also be able to explain the present isotope effects, we would like to point out that the agreement between theory and experiment should be quantitative.

**Acknowledgment:** We would like to thank A. S. Alexandrov and A. M. Bratkovsky for useful discussions. We also thank X. M. Zhang for helping with resistivity measurements. The work was supported by the NSF MRSEC at the University of Maryland and Swiss National Science Foundation.

\* Present address: Laboratoire CRISMAT-ISMRA, 14050 CAEN Cedex, France.

(1996).

- [9] G. M. Zhao, K. Conder, H. Keller, and K. A. Müller, *Nature (London)* **381**, 676 (1996).
- [10] G. M. Zhao, M. B. Hunt and H. Keller, *Phys. Rev. Lett.* **78**, 955 (1997).
- [11] S. J. L. Billinge, R. G. DiFrancesco, G. H. Kwei, J. J. Neumeier, and J. D. Thompson, *Phys. Rev. Lett.* **77**, 715 (1996).
- [12] C. H. Booth, F. Bridges, G. H. Kwei, J. M. Lawrence, A. L. Cornelius, and J. J. Neumeier, *Phys. Rev. Lett.* **80**, 853 (1998).
- [13] D. Louca, T. Egami, E. L. Brosha, H. Röder, and A. R. Bishop, *Phys. Rev. B* **56**, R8475 (1997).
- [14] A. Lanzara, N. L. Saini, M. Brunelli, F. Natali, A. Bianconi, P. G. Radelli, and S. W. Cheong, *Phys. Rev. Lett.* **81**, 878 (1998).
- [15] W. Prellier, M. Rajeswari, T. Venkatesan and R. L. Greene, *App. Phys. Lett.* **75**, 1146 (1999).
- [16] G. M. Zhao, K. Conder, H. Keller, and K. A. Müller, *Phys. Rev. B* **60**, 11 914 (1999).
- [17] R. Resel, E. Gratz, A. T. Burkov, T. Nakama, M. Higa, and K. Yagasaki, *Rev. Sci. Instrum.* **67**, 1970 (1996).
- [18] G. M. Zhao, V. Smolyaninova, W. Prellier, and H. Keller, *Phys. Rev. Lett.* **84**, 6086 (2000).
- [19] D. Emin and T. Holstein, *Ann. Phys. (N.Y.)*, **53**, 439 (1969).
- [20] I. G. Austin and N. F. Mott, *Adv. Phys.* **18**, 41 (1969).
- [21] A. S. Alexandrov and A. M. Bratkovsky, *J. Phys.: Condens. Matter*, **11**, L531 (1999).
- [22] A. S. Alexandrov and P. E. Kornilovitch, *Phys. Rev. Lett.* **82**, 807 (1999).
- [23] H. L. Ju, H. C. Sohn, and K. M. Krishnan, *Phys. Rev. Lett.* **79**, 3230 (1997).
- [24] G. J. Snyder, R. Hiskes, S. DiCarolis, M. R. Beasley, and T. H. Geballe, *Phys. Rev. B* **53**, 14434 (1996).
- [25] G. M. Zhao, V. Smolyaninova, W. Prellier, and H. Keller, *cond-mat/9912037*.
- [26] Y. Sawaki, K. Takenaka, A. Osuka, R. Shiozaki, and S. Sugai, *Phys. Rev. B* **61**, 11588 (2000).
- [27] J. M. De Teresa, M. R. Ibarra, P. A. Algarabel, C. Ritter, C. Marquina, J. Blasco, J. Garcia, A. del Moral, and Z. Arnold, *Nature (London)*, **386**, 256 (1997).

---

- [1] R. von Helmolt, J. Wecker, B. Holzapfel, L. Schultz, and K. Samwer, *Phys. Rev. Lett.* **71**, 2331 (1993); S. Jin, T. H. Tiefel, M. McCormack, R. A. Fastnacht, R. Ramesh, and L. H. Chen, *Science* **264**, 413 (1994).
- [2] A. P. Ramirez, *J. Phys.: Condens. Matter*, **9**, 8171 (1997).
- [3] C. Zener, *Phys. Rev.* **82**, 403 (1951); P. W. Anderson, and H. Hasegawa, *Phys. Rev.* **100**, 675 (1955).
- [4] A. J. Millis, P. B. Littlewood, and B. I. Shraiman, *Phys. Rev. Lett.* **74**, 5144 (1995); A. J. Millis, B. I. Shraiman, and R. Müller, *Phys. Rev. Lett.* **77**, 175 (1996).
- [5] H. Röder, J. Zang, and A. R. Bishop, *Phys. Rev. Lett.* **76**, 1356 (1996).
- [6] A. Moreo, S. Yunoki, and E. Dagotto, *Science* **283**, 2034 (1994).
- [7] A. S. Alexandrov and A. M. Bratkovsky, *Phys. Rev. Lett.* **82**, 141 (1999); A. S. Alexandrov and A. M. Bratkovsky, *J. Phys.: Condens. Matter*, **11**, 1989 (1999).
- [8] M. Jaime, M. B. Salamon, M. Rubinstein, R. E. Teece, J. S. Horwitz, and D. B. Chrisey, *Phys. Rev. B* **54**, 11914